

Supplementary Information

Cation-exchange and lateral ripening in wurtzite-like CuInSe₂ formation from weissite-like Cu_{2-x}Se

Christopher P. Pakhanyan, Allison P. Forsberg, and Richard L. Brutchey

Department of Chemistry, University of Southern California, Los Angeles, California 90089, USA.

*E-mail: brutchey@usc.edu

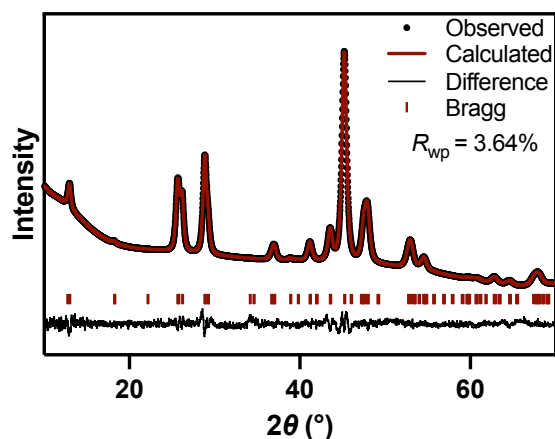


Fig. S1 Rietveld refinement of the weissite-like Cu_{2-x}Se XRD pattern using the Cu_{2-x}Te structural model (space group $P\bar{3}m1$). Experimental data were collected with $\lambda = 1.5406$ Å. Reference peaks and refinement quality indicators are shown.^{1,2}

Table S1. Crystal structure parameters of weissite-like Cu_{2-x}Se obtained by Rietveld refinement using the trigonal Cu_{2-x}Te structural model (space group $P\bar{3}m1$, No. 164).³ Lattice parameters are: $a = b = 8.016(1)$ Å, $c = 6.794(2)$ Å.

Atom	x/a	y/b	z/c
Cu	0.3333	0.6667	0.0725(56)
Cu	0.0000	0.0000	0.2800
Cu	0.4838(10)	0.5162	0.3156(25)
Cu	0.8267(14)	0.1733	0.4148(31)

Se	0.1600(13)	0.8400	0.2281(19)
Se	0.3333	0.6667	0.81(81)

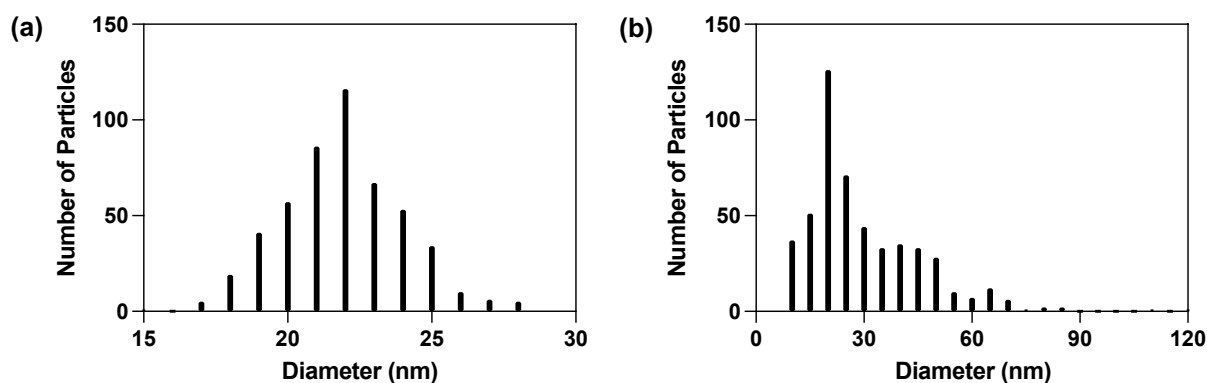


Fig. S2 Size distributions of isolated nanocrystals from reactions where no aliquots were withdrawn. (a) Weissite-like Cu_{2-x}Se , showing a narrow distribution with an average diameter of 21.9 ± 2.1 nm ($N = 500$), indicative of monodisperse nanoplates. (b) Wurtzite-like CuInSe_2 , showing a broader distribution with an average diameter of 30.1 ± 16.0 nm ($N = 500$), reflecting lateral growth and size broadening during cation exchange.

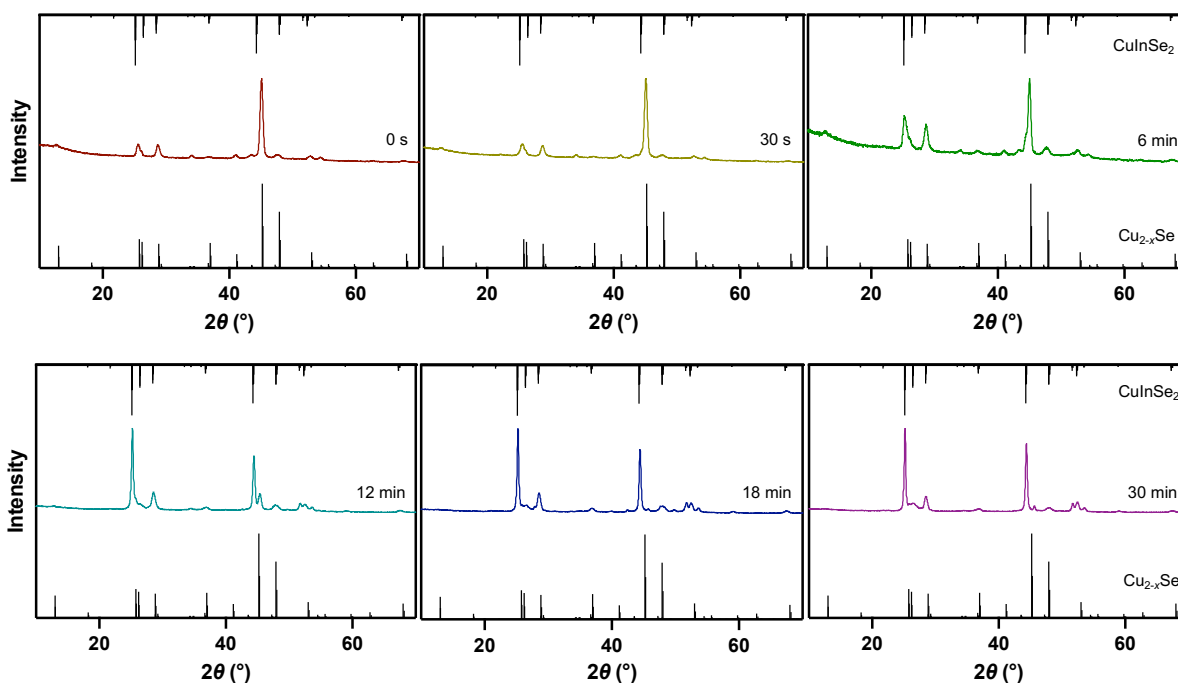


Fig. S3 Individual powder XRD patterns from Fig. 2a, showing steady structural evolution from weissite-like Cu_{2-x}Se to wurtzite-like CuInSe_2 .

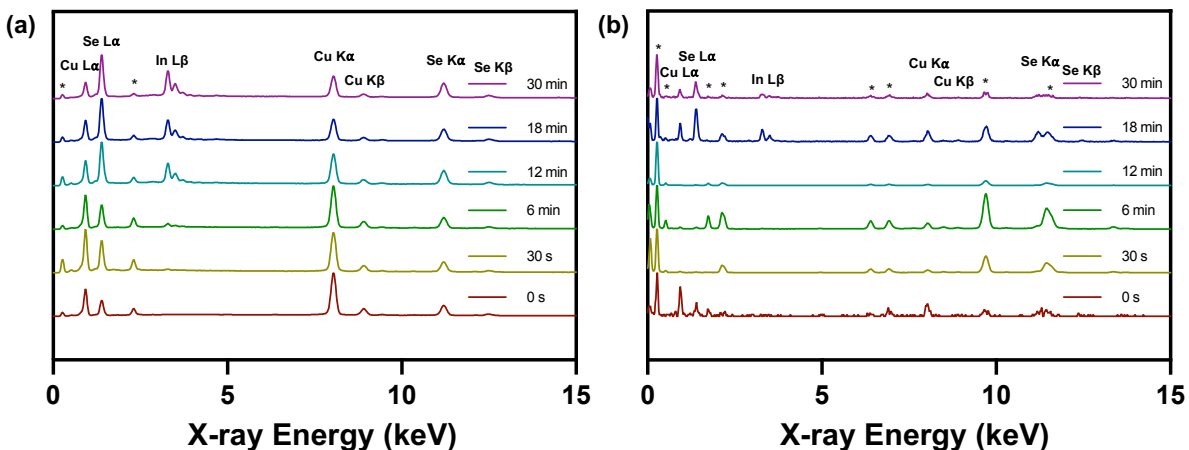


Fig. S4 EDX spectra showing steady indium incorporation over time. (a) SEM-EDX spectral data for aliquots taken from 0 s to 30 min. (b) STEM-EDX spectral data for aliquots taken from 0 s to 30 min. “*” consists of impurities coming from carbon tabs, Au TEM grids, or the TEM holder (C, Fe, S, Co, Au).

Table S2. Quantitative SEM-EDX elemental compositions of aliquots collected during the cation exchange reaction from weissite-like Cu_{2-x}Se to wurtzite-like CuInSe_2 (Fig. 2b). Values represent mean atomic percentages with standard deviations given in parentheses.

Aliquot	Cu at. %	In at. %	Se at. %
0 s	61.6(8)	0	38.4(8)
30 s	59.3(8)	1.2(2)	39.6(8)
6 min	59.4(7)	3.1(1)	37.6(6)
12 min	40.4(9)	16.9(9)	42.7(8)
18 min	34.5(3)	20.9(5)	44.5(6)
30 min	29.7(6)	23.0(12)	47.3(9)

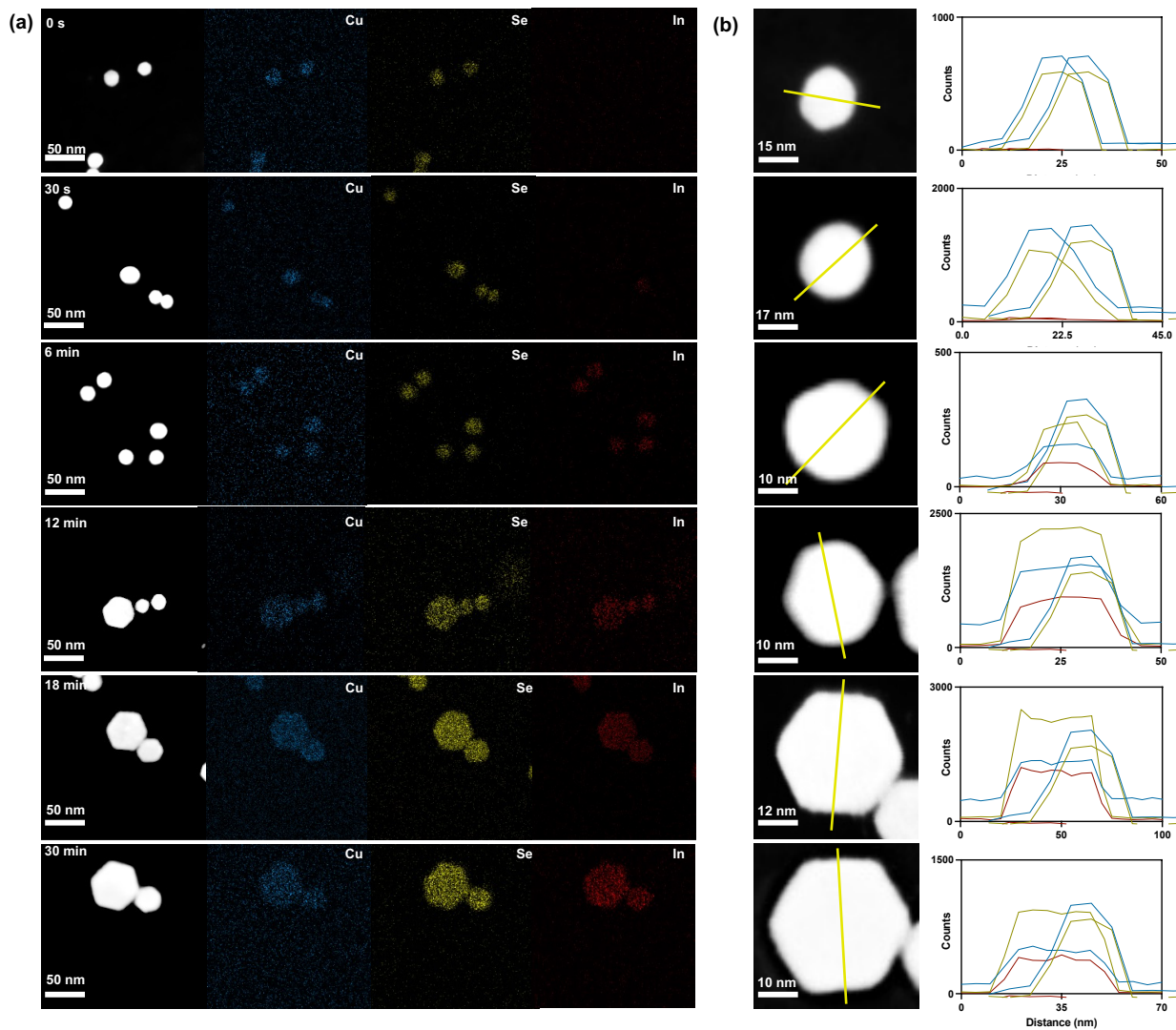


Fig. S5 STEM-EDX elemental mapping of the transformation from weissite-like Cu_{2-x}Se to wurtzite-like CuInSe_2 during a time-resolved aliquot study. (a) Aliquots were collected at 0 s, 30 s, 6 min, 12 min, 18 min, and 30 min, showing the spatial and compositional evolution of the nanocrystals. Indium incorporation proceeds isotropically across the nanocrystals over time, with minor incorporation starting at 30 s. (b) Line scan analysis emphasizing uniformity across the nanoplate diameter. *K* lines were used for Cu and *L* lines were used for Se and In.

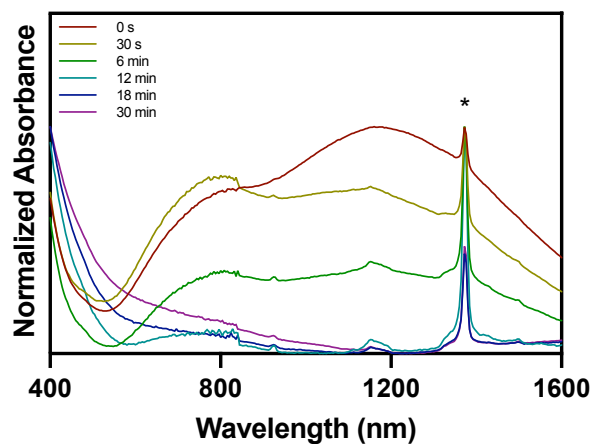


Fig. S6 UV–vis–NIR absorption spectra of aliquots collected during the reaction. The localized surface plasmon resonance of weissite-like Cu_{2-x}Se diminishes over time, while band edge features characteristic of wurtzite-like CuInSe_2 emerge.

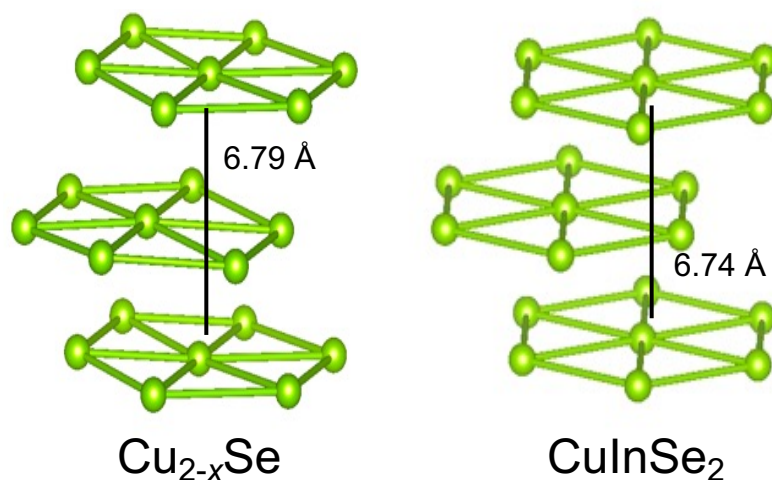


Fig. S7 Hexagonally close-packed (HCP) anion sublattices of weissite-like Cu_{2-x}Se and wurtzite-like CuInSe_2 . The interlayer spacing differs by 0.05 \AA between every other layer. Distances were determined using VESTA.

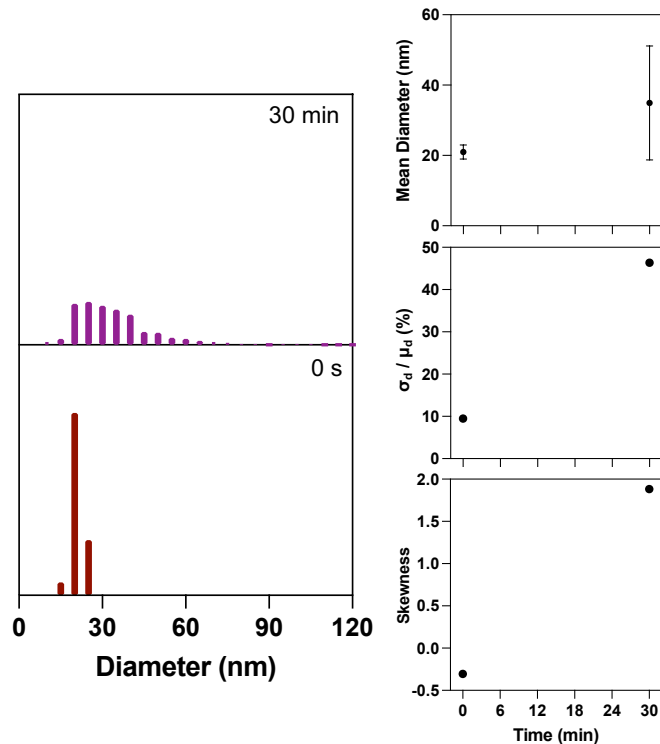


Fig. S8 Size analysis study of aliquots taken at 0 s and 30 min time points of an independent synthesis performed identically to demonstrate reproducibility. Size distribution analyses are consistent with each other, showing average particle diameters of 21.0 ± 2.0 nm and 34.9 ± 16.2 nm for Cu_{2-x}Se and CuInSe_2 , respectively. The particle size skew increases from -0.31 to 1.88, further enforcing reproducibility.

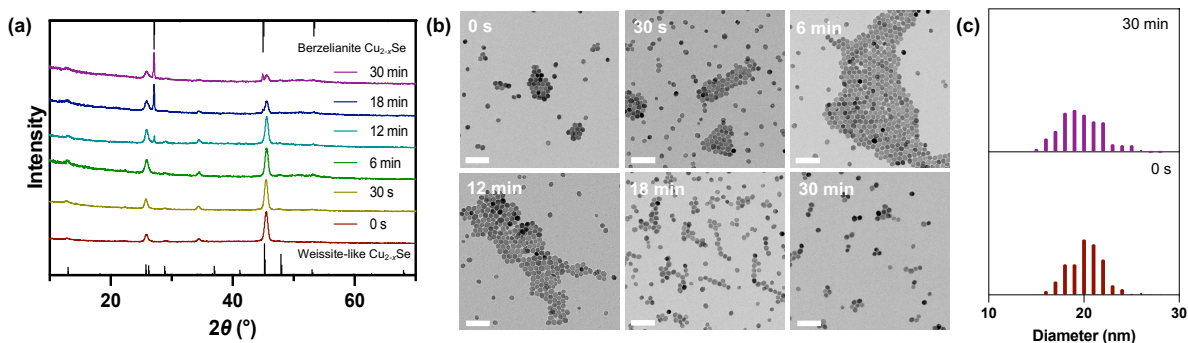


Fig. S9 (a) Aliquot study showing the structural evolution of weissite-like Cu_{2-x}Se over time in the absence of an indium source. The top stick pattern corresponds to berzelianite Cu_{2-x}Se (ICSD Coll. Code: 41143). (b) TEM images showing the hexagonal plate morphology over time; all scale bars = 100 nm. (c) Size distribution of aliquots taken at 0 s and 30 min, showing narrow distribution with average sizes of 20.2 ± 1.8 nm and 19.7 ± 2.2 nm, respectively, indicative of monodisperse nanoplates.

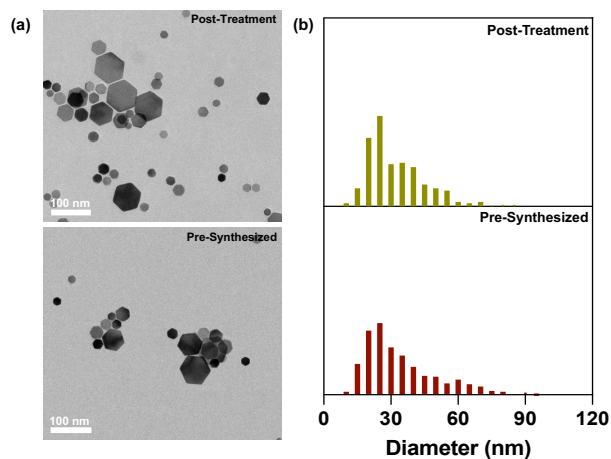


Fig. S10 Control experiment to assess ripening of the product phase in the absence of soluble precursors. (a) TEM images of pre-synthesized CuInSe_2 nanocrystals before and after re-dispersion in neat oleylamine and heat treatment under the standard cation-exchange protocol, confirming retention of the hexagonal nanoplatform morphology. (b) Size distributions ($N = 500$) before and after treatment, with mean lateral sizes of 34.2 ± 16.4 nm and 32.2 ± 13.1 nm, respectively.

References

1. N. Doebelin and R. Kleeberg, *J. Appl. Crystallogr.*, 2015, **48**, 1573–1580.
2. R. A. Young, Ed., *The Rietveld Method*, Oxford University Press Oxford, 1993.
3. L. Yu, K. Luo, S. Chen and C.-G. Duan, *CrystEngComm*, 2015, **17**, 2878–2885.